

Spectral functions of two-dimensional systems with coupling of electrons to collective or localized spin degrees of freedom

A. A. Katanin^{1,2} and V. Yu. Irkhin¹¹*Institute of Metal Physics, Kovalevskaya strasse 18, 620041 Ekaterinburg, Russia*²*Max-Planck Institut für Festkörperforschung, 70569 Stuttgart, Germany*

(Received 7 March 2006; revised manuscript received 7 November 2007; published 20 March 2008)

The spectral properties of itinerant two-dimensional systems with (nearly) ferromagnetic ground state are studied within the spin-fermion and classical s - d exchange models. While the former model describes the effect of collective magnetic excitations on the electronic properties, the latter one considers the effect of local moments. We use the equation of motion approach combined with the $1/M$ and $1/z$ expansions (M is the number of spin components and z is the coordination number) to investigate spectral functions. In both models, the spectrum splitting occurs at low temperatures T in the renormalized classical regime due to strong magnetic fluctuations. For the interaction J between electronic and magnetic degrees of freedom comparable to the bandwidth (the intermediate-coupling regime), the $1/z$ expansion predicts full splitting of electronic spectrum or opening the magnetically induced gap below some temperature T_s . At the same time, the spectrum remains only partly split in the $1/M$ expansion with the quasiparticle structure, which becomes fully coherent at low T .

DOI: [10.1103/PhysRevB.77.115129](https://doi.org/10.1103/PhysRevB.77.115129)

PACS number(s): 71.10.Fd, 71.10.Hf, 71.27.+a, 71.30.+h

I. INTRODUCTION

The narrow-band d systems pose the problem of magnetism of electronic systems, where the electron-electron interactions are comparable to the bandwidth. Two different points of view on magnetic excitations in such systems can be considered. On one hand, magnetic excitations can be treated as collective excitations of itinerant electrons.¹ On the other hand, in many d - and especially f -electron systems, one can consider localized (magnetic) and itinerant excitations as two independent degrees of freedom interacting with each other.

The latter viewpoint is convenient, e.g., for transition metals containing both conducting and localized electrons. For the description of such systems, the s - d exchange model was introduced about 50 years ago by Vonsovskii.² The corresponding one-impurity model was applied later for the explanation of the Kondo effect;³ the periodic version of this model (the Kondo lattice model) was used for the description of the anomalous properties of strongly correlated f -electron systems, e.g., heavy-fermion compounds.⁴ The strong-coupling (“double-exchange”) limit of the s - d model was applied for treating the interaction between localized moments and current carriers in a narrow d band in ferromagnetic semiconductors⁵ (e.g., chalcogenide spinels) and manganates.^{6,7}

The strong interaction between the itinerant and localized degrees of freedom in the above-mentioned class of systems can lead to incoherent structures in the spectral functions, in particular, the gap in electronic spectrum can arise due to local correlations. Such a situation occurs, e.g., in the s - d exchange model, which shows a metal-insulator transition with increasing the interaction of localized spins with conduction electrons in a half-filled band due to the alignment of spins of conduction electrons along the local spins, reducing the number of doubly occupied sites.^{8,9} This transition is similar to the metal-insulator transition studied for the half-filled Hubbard model¹⁰ and was investigated within the extended dynamical mean-field theory.¹¹ In more than three

dimensions, the local $d \rightarrow \infty$ picture^{10,11} is expected to give a qualitatively correct description of the physics near the metal-insulator transition, while the situation in three dimensions may be more involved. In particular, it was proposed that the appreciable short-range magnetic order in $d=3$ may lead to the magnetic spin splitting above the Curie temperature T_C .^{12,13} Such a splitting, which cannot be described within the local theory, was presumably observed in strong itinerant magnets Fe and Ni.¹⁴

At the same time, in the peculiar $d=2$ (or quasi-two-dimensional) case which is physically relevant for the layered magnetic systems with small interlayer hopping (layered manganites, cuprates, and other compounds with the perovskite structure), the strong short-range magnetic order takes place. It is especially pronounced in the so-called renormalized classical temperature regime, which arises above the magnetically ordered ground state and is characterized by an exponentially large correlation length $\xi \propto \exp(A/T)$ (A is some constant).¹⁵ Strong magnetic correlations in this regime result in the structure of the electronic spectrum, which is similar to that in the ordered phase.^{16–18} As a result, a quasisplitting of the Fermi surfaces or a pseudogap can occur at low enough temperatures due to ferromagnetic¹⁹ (FM) or antiferromagnetic (AFM)/charge density wave (CDW) fluctuations.²⁰ These features of spectral functions have a clearly different nature as compared to the above discussed Mott gap, since the finite ($d=2$) dimension is crucial for their appearance; they are also expected to be relevant for quasi-two-dimensional (quasi-2D) systems with small interlayer hopping above the magnetic transition temperature.

Recently, the pseudogap structures have been observed in layered manganite compound $\text{La}_{1.2}\text{Sr}_{1.8}\text{Mn}_2\text{O}_7$.²¹ These structures are present both above and below T_C , and possibly originate from the CDW fluctuations.⁷ The FM fluctuations, however, may be responsible for the part of the pronounced shift (~ 250 meV) of the spectral weight maxima off the Fermi level above the Curie temperature.

The separation of conduction and localized magnetic degrees of freedom can be also “dynamic” and arise in purely itinerant electronic systems due to strong short-range magnetic order. In particular, it was pointed out that even purely itinerant electronic systems in the regime of strong magnetic correlations can be described by an effective classical s - d model.¹⁸

To treat the effect of collective magnetic degrees of freedom on the electronic properties and describe properties of 2D systems near magnetic quantum phase transitions, another model, *spin-fermion model*, was introduced.^{22–24} Although this model was originally proposed as a phenomenological model for systems with strong AFM fluctuations, the systems with strong FM fluctuations can be treated within this model as well.^{25,26}

The comparison of the spectral properties of systems where magnetic fluctuations are induced by local moments (described within the s - d model) or collective magnetic fluctuations (described within the spin-fermion model) in the regime of strong magnetic fluctuations is of certain interest. The spectral properties of the 2D systems with strong magnetic fluctuations were investigated previously within the spin-fermion model in the Eliashberg approximation,^{24,25} which neglects vertex corrections, and in the quasistatic approach, performing summation of all the types of diagrams, but neglecting the effect of dynamic spin fluctuations.^{23,26} The latter approach yields the two-peak structure of the spectral function for both strong FM and AFM correlations, with a finite spectral weight at the Fermi level at finite ξ .

Contrary to the spin-fermion model, where the length of the spin vector describing magnetic degrees of freedom at each lattice site is not fixed, the s - d model considers fixed spin length. The result for the spectral weight $A(\mathbf{k}_F, \nu) \sim \nu^2$ in the zero-bandwidth limit of the spin-fermion model^{23,26} shows that the spectral weight vanishes at $\nu=0$ only, and a true metal-insulator transition is not expected to occur. Such a transition is, however, expected to be described by the s - d model.^{9,27,28} Treating of electronic properties near this transition is reminiscent of the problem of considering the effect of magnetic fluctuations in a strongly correlated Hubbard model. Although a number of approaches were proposed recently which extend the $d \rightarrow \infty$ dynamical mean-field theory¹⁰ (DMFT) to account for the short-range²⁹ and long-range^{30–33} correlations, the development of analytical approaches to this problem is also of certain interest.

To study the magnetic fluctuations in the regime of the intermediate and strong interactions between localized and itinerant subsystems, the $1/z$ expansion, where z is the coordination number, can be used. This approach has been applied before to the ferro- and paramagnetic s - d models (see Refs. 8, 9, 27, and 28) as well as to the paramagnetic state in the Hubbard model.^{9,34} Its extension to describe the paramagnetic state with strong magnetic correlations is of certain interest.

Another promising candidate for nonperturbative description of strongly correlated electronic systems is the Ward-identity approach.³⁵ Although this approach was quite successful in describing the strongly FM ordered state,³⁶ its generalization to the weak FM and paramagnetic situations meets difficulties, since the contribution of longitudinal spin

fluctuations, which should be taken into account in these cases, makes the system of equations for the electronic self-energy and electron-(para)magnon vertices not closed.

This difficulty was overcome in a recently proposed combination of the Ward-identity approach with the $1/M$ expansion¹⁹ (M is the number of spin components; $M=3$ for the s - d and Hubbard models). The use of the $1/M$ expansion gives a possibility to truncate the hierarchy of integral equations for the self-energy and electron-magnon vertices. To apply this method to a broader class of models, we consider in the present paper its generalization—the equation of motion approach combined with the $1/M$ expansion. Contrary to the $1/z$ expansion, which considers equations of motion for Hubbard operators, this method is applied to fermionic operators, which allows us to describe both weak- and strong-coupling regimes, as well as the crossover between them.

The plan of the paper is the following. In Sec. II, we present the theoretical models describing the interaction of electronic and magnetic degrees of freedom in strongly correlated systems. In Sec. III, we formulate the $1/z$ expansion for the s - d model. In Sec. IV, we use the equation of motion method to derive the self-consistent equations for the self-energy and electron-magnon vertices within the $1/M$ expansion, the details of the derivation being presented in the Appendix. In Sec. V, we investigate the electronic self-energy, spectral functions, and electron-magnon vertices in different regimes. Finally, in Sec. VI, we summarize the main results of the paper.

II. MODEL

We consider a correlated electronic system with itinerant and localized-moment subsystems, which is described by the generating functional

$$Z[\eta] = \int D[c, c^\dagger] D[\mathbf{S}] \exp\{-\mathcal{S}[c, \mathbf{S}]/T - (c_{k\sigma}^\dagger \eta_{k\sigma} + \eta_{k\sigma}^\dagger c_{k\sigma})\}, \quad (1)$$

where the fields c and \mathbf{S} correspond to the electronic and spin degrees of freedom, respectively. The action $\mathcal{S}[c, \mathbf{S}]$ has the form

$$\begin{aligned} \mathcal{S}[c, \mathbf{S}] = & iT \int_0^{1/T} d\tau \sum_i \mathbf{A}(\mathbf{S}_i) \frac{\partial \mathbf{S}_i}{\partial \tau} + \sum_k (i\nu_n - \varepsilon_{\mathbf{k}}) c_{k\sigma}^\dagger c_{k\sigma} \\ & + \sum_q \mathcal{R}_q \mathbf{S}_q \mathbf{S}_{-q} + J \sum_{kk'\sigma\sigma'} \mathbf{S}_{k-k'} \boldsymbol{\sigma}_{\sigma\sigma'} c_{k\sigma}^\dagger c_{k'\sigma'}, \end{aligned} \quad (2)$$

where the first three terms describe the electronic and spin subsystems, the last term proportional to J corresponds to the interaction between them, $q=(\mathbf{q}, i\omega_n)$, $k=(\mathbf{k}, i\nu_n)$, $\omega_n=2n\pi T$ and $\nu_n=(2n+1)\pi T$ are bosonic and fermionic Matsubara frequencies, $\varepsilon_{\mathbf{k}}$ is the electronic spectrum, $\boldsymbol{\sigma}_{\sigma\sigma'}$ are the Pauli matrices, and the term proportional to \mathcal{R}_q describes an indirect spin-spin exchange. Below, we suppose that this exchange is ferromagnetic, i.e., $\mathcal{R}_{\mathbf{q},0}$ has its minimum at $\mathbf{q}=0$.

Two different versions of the model (2) are considered in the paper. The first version, which is referred to as “ s - d type

models," has the measure of integration over the field \mathbf{S}

$$D[\mathbf{S}] = D_{\text{sd}}[\mathbf{S}] \equiv \prod_i \delta(\mathbf{S}_i^2 - S^2) d^3\mathbf{S}_i, \quad (3)$$

so that the length of the field \mathbf{S} is fixed to S . This is, in particular, the case for the lattice analog of the standard s - d exchange model² (i.e., Kondo-lattice model). In this case, the vector potential $\mathbf{A}(\mathbf{S})$ describes the precession of free spin and satisfies the equation $\nabla_S \times \mathbf{A}(\mathbf{S}) \cdot \mathbf{S} = 1$, $\nabla_S = (\partial/\partial S_x, \partial/\partial S_y, \partial/\partial S_z)$. In the classical limit $S \rightarrow \infty$, this term fixes the field \mathbf{S} to be static, $\partial\mathbf{S}/\partial\tau = 0$ (cf. Ref. 37). For the s - d type of models, the term proportional to \mathcal{R}_q in Eq. (2) can be considered as arising, e.g., from the indirect spin-spin Ruderman-Kittel-Kasuya-Yosida exchange.

The model (2) with $D[\mathbf{S}] = D_{\text{sd}}[\mathbf{S}]$ and $\mathbf{A}(\mathbf{S}) = 0$ (which is referred to as an effective s - d model in the following) can be naturally obtained from the Hubbard model in the renormalized classical regime.¹⁸ The quantity \mathcal{R}_q is determined in this mapping by the random-phase approximation expression for the inverse susceptibility in the ordered phase.¹⁸

Another version of the model (2) we consider is the spin-fermion model²²⁻²⁴ with

$$D[\mathbf{S}] = \prod_i d^3\mathbf{S}_i, \quad \mathbf{A}(\mathbf{S}) = 0. \quad (4)$$

Contrary to the s - d model, the field \mathbf{S} describes, in this case, three *independent* Bose-like fields, i.e., corresponding operators $\hat{\mathbf{S}}_q^a$ with different a commute with each other. The spin-fermion model can be also considered as that representing the low-energy electron and spin excitations of the Hubbard model in the quantum-critical regime.^{24,38} The quantity \mathcal{R}_q corresponds, in this case, to the inverse susceptibility χ_q^{-1} and enters as a phenomenological input parameter of the spin-fermion model.

Both the static case $\partial\mathbf{S}/\partial\tau = 0$ and the case $\mathbf{A}(\mathbf{S}) = 0$ allow the generalization of the model (2) to M -component spins $\mathbf{S}_i = (S_i^1, \dots, S_i^M)$. This generalization will be used throughout the paper to perform the $1/M$ expansion of the self-energy and electron-magnon vertices.

For purely static $\mathcal{R}_q = \delta_{n0}\mathcal{R}_q$, the s - d and spin-fermion models are described by the Hamiltonian

$$H = \sum_{\mathbf{k}} \varepsilon_{\mathbf{k}} \hat{c}_{\mathbf{k}\sigma}^\dagger \hat{c}_{\mathbf{k}\sigma} + \sum_{\mathbf{q}} \mathcal{R}_q \hat{\mathbf{S}}_{\mathbf{q}} \hat{\mathbf{S}}_{-\mathbf{q}} + H_{\text{int}}, \quad (5)$$

$$H_{\text{int}} = -J \sum_{\mathbf{k}\mathbf{k}'} \hat{\mathbf{S}}_{\mathbf{k}-\mathbf{k}'} \sigma_{\sigma\sigma'} \hat{c}_{\mathbf{k}\sigma}^\dagger \hat{c}_{\mathbf{k}'\sigma'}$$

Here, the Fourier transformed operators $\hat{\mathbf{S}}_i$, which correspond to the fields \mathbf{S}_i in the continuum integral formalism, obey the standard $SU(2)$ commutation relations and the condition $\hat{\mathbf{S}}^2 = S(S+1)$ for the s - d model, while the components of $\hat{\mathbf{S}}$ commute with each other and $\hat{\mathbf{S}}^2$ is not fixed for the spin-fermion model. In the present paper, we discuss only the classical limit of the s - d model with commuting $\hat{\mathbf{S}}$ operators, so that the difference between these two models is only in the additional restriction for the $\hat{\mathbf{S}}^2$ for the s - d model (the quantum s - d model with the noncommuting spin operators will be

considered elsewhere). For definiteness, we assume $J > 0$; the results in the classical limit are the same for positive and negative J .

III. $1/z$ EXPANSION FOR THE s - d MODEL

The $1/z$ expansion considers perturbation theory around the atomic limit of the model ($\varepsilon_{\mathbf{k}} = \text{const}$). The corresponding sequence of equations of motion for the electronic Green's function was considered in Refs. 9 and 27. To zeroth order in $1/z$, we obtain the result of the Hubbard-I approximation

$$G_{\mathbf{k}}(\nu) = \frac{1}{F_0(\nu) - \varepsilon_{\mathbf{k}}}, \quad (6)$$

where $F_0(\nu) = \nu - I^2/\nu$ and $I = JS$. To first order in $1/z$, one has to replace $F_0(\nu) \rightarrow F_{\mathbf{k}}(\nu)$, where

$$F_{\mathbf{k}}(\nu) = \nu \left[1 + \frac{J^2 MT}{\nu} \sum_{\mathbf{q}} \frac{\chi_{\mathbf{q}}}{F_0(\nu) - \varepsilon_{\mathbf{k}+\mathbf{q}}} \right]^{-1} \quad (7)$$

and $\chi_{\mathbf{q}}$ is the nonuniform static spin susceptibility of the model (5). Despite that the result (7) is obtained within the strong-coupling expansion of the s - d model, it reproduces correctly in second order in J the corresponding perturbation theory result for the electronic self-energy.⁸

The result (7) does not guarantee, however, correct analytical properties of the electronic Green's function at arbitrary J . To obtain analytical results, we consider self-consistent approximation of Hubbard-III type^{9,27}

$$F_{\mathbf{k}}(\nu) = \nu \frac{1 + [F_0(\nu) - F_{\mathbf{k}}(\nu)] \tilde{G}_{\mathbf{k}}(\nu)}{1 + [\nu - F_{\mathbf{k}}(\nu)] \tilde{G}_{\mathbf{k}}(\nu)}, \quad (8)$$

where

$$\tilde{G}_{\mathbf{k}}(\nu) = \frac{MT}{S^2} \sum_{\mathbf{q}} \frac{\chi_{\mathbf{q}}}{F_{\mathbf{k}}(\nu) - \varepsilon_{\mathbf{k}+\mathbf{q}}}. \quad (9)$$

The solution of Eq. (8) yields

$$F_{\mathbf{k}}(\nu) = \nu + \frac{1 - \sqrt{1 + 4I^2 \tilde{G}_{\mathbf{k}}^2(\nu)}}{2\tilde{G}_{\mathbf{k}}(\nu)}. \quad (10)$$

The result for the electronic self-energy $\Sigma_{\mathbf{k}}(\nu) = \nu - F_{\mathbf{k}}(\nu)$, obtained from Eq. (10) with $\chi_{\mathbf{q}} = S^2/T$, coincides with the result of the solution of single-impurity model of the DMFT for the classical s - d model, Eq. (9) serving then as a self-consistency condition.

IV. SELF-CONSISTENT EQUATIONS FOR THE SELF-ENERGY AND VERTICES WITHIN THE $1/M$ EXPANSION

To find the electronic self-energy in model (5) within the $1/M$ expansion, we consider the equation of motion for the fermionic operator $\hat{c}_{\mathbf{k}\sigma}(\tau)$ in the Heisenberg representation (see, e.g., Ref. 39)

$$(\partial/\partial\tau + \varepsilon_{\mathbf{k}})\hat{c}_{\mathbf{k}\sigma}(\tau) = [H_{\text{int}}, \hat{c}_{\mathbf{k}\sigma}](\tau) = J \sum_{\mathbf{k}'\sigma'} \boldsymbol{\sigma}_{\sigma\sigma'} \hat{\mathbf{S}}_{\mathbf{k}-\mathbf{k}'}(\tau) \hat{c}_{\mathbf{k}'\sigma'}(\tau). \quad (11)$$

Applying this equation to the electronic Green's function, we find the expression for the electronic self-energy

$$\Sigma_{\mathbf{k}} = \frac{1}{J} \sum_q' (\Gamma_{\mathbf{k};q}^z + \Gamma_{\mathbf{k};q}^\perp) G_{\mathbf{k}+q}^0, \quad (12)$$

where we have used the notation

$$\sum_q' \equiv T J^2 \sum_{\mathbf{q}} \sum_{i\omega_n}.$$

The vertices Γ describe scattering of an itinerant electron by the magnetic excitation (cf. Ref. 35),

$$\Gamma_{\mathbf{k};q}^m = \int d\tau_1 d\tau_2 e^{i\nu_n(\tau_1-\tau_2)+i\omega_n\tau_2} \langle T[\hat{c}_{\mathbf{k}\sigma}^\dagger(\tau_1) \hat{c}_{\mathbf{k}+q\sigma}(\tau_2) \hat{S}_{\mathbf{q}}^m(0)] \rangle \times G_{\mathbf{k}}^{-1} (G_{\mathbf{k}+q}^0)^{-1}, \quad (13)$$

$T[\dots]$ stands for the imaginary-time ordering, $G_{\mathbf{k}}^0$ and $G_{\mathbf{k}}$ are the bare and full fermionic Green's functions, respectively, and $m=+, -, \text{ or } z$. Note that despite the similarity of the definition of the vertex (13) with that used for the Hubbard model in Ref. 35, $\hat{S}_{\mathbf{q}}^m$ denotes, in our case, the spin-subsystem operator rather than the spin-density operator of itinerant electrons.

The vertices (13) can be found by applying equation of motion (11) once more. For the following consideration, it is convenient to introduce the corresponding one-particle irreducible vertex with amputated bosonic and fermionic leg (cf. Ref. 35)

$$\gamma_{\mathbf{k};q}^m = G_{\mathbf{k}+q}^0 \Gamma_{\mathbf{k};q}^m (J \chi_{\mathbf{q}}^m G_{\mathbf{k}+q}), \quad (14)$$

where $\chi_{\mathbf{q}}^m$ is the dynamic spin susceptibility. The equation of motion relates the vertices (14) to the one-particle irreducible vertices of the interaction of the electron with two (para) magnons. This vertex is, in turn, related to the vertex of an electron interaction with three paramagnons and so on (see Appendix for additional details). In the following, we denote the vertex of an interaction of an electron with n paramagnons as $\gamma_{\mathbf{k};q_1\dots q_n}^{m_1\dots m_n}$, where $m_i=+, -, \text{ and } z$ are the paramagnon spin indices, \mathbf{k} is the vector of the incoming fermion momentum and frequency, and $q_1\dots q_n$ are the vectors of the paramagnon momenta and frequencies. To truncate the resulting hierarchy of equations for the vertices, we follow the approach of Ref. 19 and retain only the terms which contribute to the self-energy in the zeroth and first order in $1/M$ (see the Appendix).

The resulting system of equations for the self-energy and vertices reads

$$\Sigma_{\mathbf{k}} = M \sum_q' \gamma_{\mathbf{k}+q} G_{\mathbf{k}+q} \chi_{\mathbf{q}},$$

$$\gamma_{\mathbf{k}} = 1 + \sum_q' [(2-M) \gamma_{\mathbf{k}+q}^2 G_{\mathbf{k}+q}^2 + \gamma_{\mathbf{k}+q}^{zz} G_{\mathbf{k}+q}] \chi_{\mathbf{q}},$$

$$\gamma_{\mathbf{k}}^{zz} = M \sum_q' [2 \gamma_{\mathbf{k}+q}^3 G_{\mathbf{k}+q}^3 + \gamma_{\mathbf{k}+q} \gamma_{\mathbf{k}+q}^{zz} G_{\mathbf{k}+q}^2 + \gamma_{\mathbf{k}+q}^{zz\perp} G_{\mathbf{k}+q}] \chi_{\mathbf{q}} + \alpha \gamma_{\mathbf{k}} G_{\mathbf{k}},$$

$$\gamma_{\mathbf{k}}^{zz\perp} = -2M \sum_q' [\gamma_{\mathbf{k}+q}^4 G_{\mathbf{k}+q}^4 + \gamma_{\mathbf{k}+q}^2 \gamma_{\mathbf{k}+q}^{zz} G_{\mathbf{k}+q}^3 + \gamma_{\mathbf{k}+q} \gamma_{\mathbf{k}+q}^{zz\perp} G_{\mathbf{k}+q}^2] \chi_{\mathbf{q}} - \alpha \gamma_{\mathbf{k}}^2 G_{\mathbf{k}}^2, \quad (15)$$

where $G_{\mathbf{k}} = [i\nu_n - \varepsilon_{\mathbf{k}} - \Sigma_{\mathbf{k}}]^{-1}$ is the full (dressed) electronic Green's function, $\gamma_{\mathbf{k}}^{m_1\dots m_n} = \gamma_{\mathbf{k};0\dots 0}^{m_1\dots m_n}$ are the electron-paramagnon vertices at zero paramagnon momenta, $\gamma_{\mathbf{k}} = \gamma_{\mathbf{k};0}^z$, $\chi_{\mathbf{q}} = \chi_{\mathbf{q}}^z$, $\alpha=0$ for the spin-fermion model, and $\alpha=-2$ for the s - d model.

Comparing Eqs. (15) with the result (10) of the $1/z$ expansion, we see that these expansions treat vertex corrections in different ways. While the $1/M$ expansion treats accurately the momentum dependence of the vertices, the ‘‘average’’ vertex of the $1/z$ expansion $[\sqrt{1+4I^2\tilde{G}_{\mathbf{k}}^2(\nu)}-1]/[2I^2\tilde{G}_{\mathbf{k}}^2(\nu)]$ interpolates between the weak- and strong-coupling regimes. Both approaches, however, are expected to be applicable in the weak- and intermediate-coupling regimes. Below, we consider the result of application of these approaches to the calculation of spectral functions in the s - d and spin-fermion models.

V. RESULTS FOR THE SPECTRAL FUNCTIONS, SELF-ENERGY, AND VERTICES

Equations (15) give a possibility to investigate the evolution of the spectral properties with varying electron-spin coupling J and the strength of magnetic correlations. For practical calculations, one has to specify an explicit form of the magnetic susceptibility $\chi_{\mathbf{q}}$. In the following, we consider the low-temperature regime with strong magnetic fluctuations, where we employ an ansatz

$$\chi_{\mathbf{q}} = \frac{1}{M} \frac{A}{\mathbf{q}^2 + \xi^{-2}} \delta_{n0}, \quad |\mathbf{q}| \ll 1 \quad (16)$$

for the classical s - d exchange model and

$$\chi_{\mathbf{q}} = \frac{1}{M} \frac{A}{\mathbf{q}^2 + \xi^{-2} + r|\omega_n|/|\mathbf{q}|}, \quad |\omega_n|/v_F \ll |\mathbf{q}| \ll 1 \quad (17)$$

for the effective s - d and spin-fermion models (we have picked out explicitly the factor $1/M$ for further convenience). While the constant A is determined by the stiffness of spin excitations and can be arbitrary, the correlation length ξ for the s - d type models is chosen to fulfill the sum rule

$$MT \sum_q \chi_{\mathbf{q}} = S^2. \quad (18)$$

For the spin-fermion model, the correlation length is an independent parameter, which, however, can be related to the quantity Δ according to

$$MT \sum_{\mathbf{q}} \chi_{(\mathbf{q},0)} = (\Delta/J)^2. \quad (19)$$

For the ferromagnetically ordered ground state, Δ is expected to be almost temperature independent at low T . We also con-

sider the high-temperature regime with $\chi_q = S^2/(MT)\delta_{n0}$.

Note that the ansatz (16) and (17) neglects the nonanalytical corrections to the spin susceptibility,⁴¹ which are expected to be not too important in the renormalized classical regime.

A. $T=0$ and high-temperature results

We start investigating the solutions of Eqs. (9) and (15) from the $\xi \rightarrow \infty$ ($T \rightarrow 0$) limit. In this case, the dominant contribution to momenta sums comes from the vicinity of $q=0$ point. Neglecting the momentum and frequency transfer q in the Green's functions and the vertices in Eqs. (9) and (15), we obtain for the s - d model in both $1/z$ and $1/M$ expansions,

$$\Sigma_k = \frac{I^2}{\bar{\nu}}, \quad \gamma_k = 1 - \frac{I^2}{\bar{\nu}^2}, \quad (20)$$

where $\bar{\nu} = \nu - \varepsilon_{\mathbf{k}} + i0$. The result (20) with $\bar{\nu} = \nu$ coincides with that in the atomic limit of the classical s - d model, where the spin dynamics can, indeed, be neglected and there are two energy levels at $\nu = \pm I$ for parallel and antiparallel orientation of the spins of itinerant electron and localized moment. In the $\xi \rightarrow \infty$ case, the two poles of the Green's function correspond to the splitting of the Fermi surface by strong magnetic fluctuations to Fermi surfaces of quasiparticles with different spin projection.

The result (20) can be compared to the corresponding result of the $1/M$ expansion for the spin-fermion model:¹⁹

$$\Sigma_k = \frac{M(\Delta_0^2 + \bar{\nu}^2 - \sqrt{\bar{\nu}^2 - \alpha_1 \Delta_0^2} \sqrt{\bar{\nu}^2 - \alpha_2 \Delta_0^2})}{2(2+M)\bar{\nu}},$$

$$\gamma_k = \frac{M}{2(2+M)^2 \Delta_0^2 \bar{\nu}^2} [2\bar{\nu}^4 + (6+M)\Delta_0^2 \bar{\nu}^2 - M\Delta_0^4 + (M\Delta_0^2 - 2\bar{\nu}^2) \sqrt{\bar{\nu}^2 - \alpha_1 \Delta_0^2} \sqrt{\bar{\nu}^2 - \alpha_2 \Delta_0^2}], \quad (21)$$

where $\Delta_0 = \Delta(T \rightarrow 0)$ and $\alpha_{1,2} = 1 + 4(1 \pm \sqrt{1+M/2})/M$; the branch $\text{Im} \sqrt{z} \geq 0$ of the square roots is chosen to guarantee the correct analytical properties for Σ and γ . The result (21) yields also the two-peak structure of the spectral function with peaks at $\nu \simeq \pm \Delta_0$ and a finite gap $\Delta_{sf} \sim \Delta_0/2$ at the Fermi level. As discussed in Refs. 19 and 26, the finite gap in the spectral function in this case is, however, an artifact of the first-order approximation in $1/M$, since the actual spectral function in the atomic limit has a behavior at small frequencies $A(\nu) \sim |\nu|^{M-1}$, which is nonanalytic in $1/M$ (see Refs. 23 and 26). However, as will be shown below, the gap disappears quickly at finite ξ , making the situation, in this case, more favorable for the application of $1/M$ expansion.

Now, we study the solutions to Eqs. (15) at finite ξ (and T). At high temperatures, the correlation length is small and the q dependence of the magnetic susceptibility can be neglected, $\chi_q = S^2/(MT)\delta_{n0}$. The criterion for this behavior is $T \gg J^2/v_F$ for the s - d exchange model and $T \gg v_F$ for the spin-fermion model (v_F is the Fermi velocity). The latter criterion is never fulfilled in real systems (which is a consequence of the fact that the local moments are not formed in the spin-fermion model, i.e., the magnetism formation

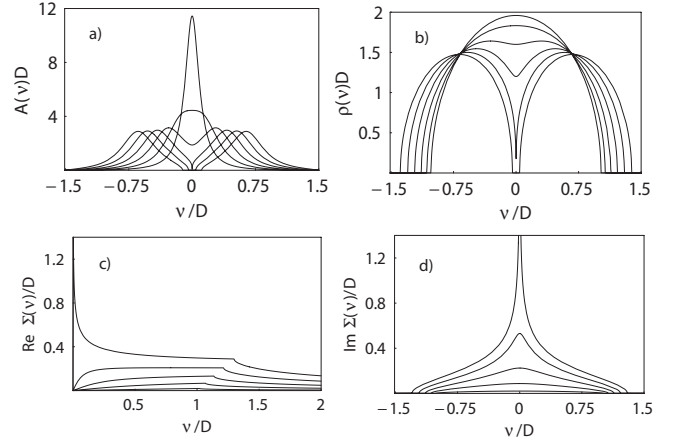


FIG. 1. (a) The spectral functions, (b) the interacting density of states $\rho(\nu)$, and (c) real and (d) imaginary parts of the self-energy of the s - d model in the high-temperature regime at $I=0.1nD$, [(a) and (b)] $n=1, \dots, 5$ (from below to above), (c) $n=2, \dots, 7$, and (d) $n=1, \dots, 6$ (from above to below).

mechanism is essentially Stoner-like), so that we consider the s - d model only. In the above-mentioned limit, we obtain in the $1/z$ expansion

$$\Sigma_\nu = [\sqrt{1 + 4I^2(G_\nu^{\text{loc}})^2} - 1]/(2G_\nu^{\text{loc}}), \quad (22a)$$

$$G_\nu^{\text{loc}} = \int_{-\infty}^{\infty} \rho_0(\nu')(\nu - \nu' - \Sigma_\nu)^{-1}, \quad (22b)$$

where $\rho_0(\nu)$ is the noninteracting density of states for the dispersion $\varepsilon_{\mathbf{k}}$. As mentioned in Sec. III, Eq. (22a) coincides with the solution of the corresponding impurity model of DMFT, while Eq. (22b) is the self-consistency condition. The result (22) is correctly reproduced by the $1/M$ expansion in the $d \rightarrow \infty$ limit, which is obtained by replacing the nonlocal Green's functions by the local one, $G_\nu^{\text{loc}} = \Sigma_{\mathbf{k}} G_{\mathbf{k}}$. At finite d , this expansion leads, however, to more complicated equations, which we do not consider in this paper.

The evolution of the self-energy Σ_ν , the spectral function at the Fermi surface $A(\nu) = -\text{Im} G_{\mathbf{k}_F, \nu}/\pi$, and the density of states $\rho(\nu) = -\text{Im} G_\nu^{\text{loc}}/\pi$ with increasing I calculated according to Eqs. (22a) and (22b) for the Bethe (semielliptic) bare density of states $\rho_0(\nu) = 2\sqrt{D^2 - \nu^2}/(\pi D^2)$ is shown in Fig. 1 (D is half of the bandwidth). Although the spectral functions have a one-peak structure at small enough I , one can observe that the quasiparticle picture is, in fact, invalid at arbitrarily small I since the real part of the self-energy has a positive slope and $|\text{Im} \Sigma_\nu|$ is maximum at the Fermi level. These features are very similar to those observed earlier in the spin-fermion model in the presence of strong magnetic correlations,²⁶ although their physical origin in the present case is different. Above a critical value $I > I_c = 0.5D$, both the real and imaginary parts of the self-energy diverge at the Fermi level and the spectral functions have the two-peak structure. The density of states $\rho(\nu)$ acquires a gap at the Fermi level above I_c , which corresponds to a metal-insulator transition.

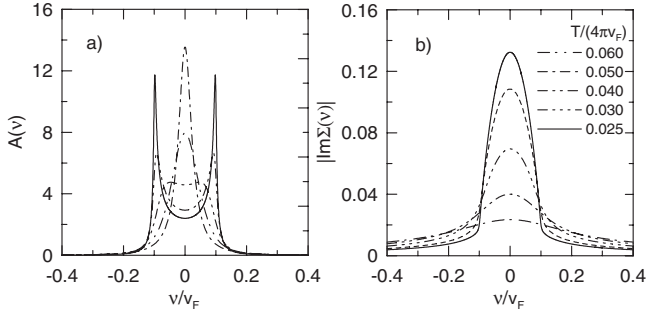


FIG. 2. (a) Spectral functions and (b) the imaginary part of the self-energy of the classical s - d model in the weak-coupling regime ($I=0.1v_F, D=5v_F$) at different low temperatures within the $1/z$ expansion.

B. Low-temperature results in the weak-coupling regime

Now, we investigate the low-temperature regime with large correlation length ξ and the susceptibility ansatz (16) or (17). First, we consider the contribution of the static spin fluctuations with zero bosonic Matsubara frequencies $\omega_n=0$ only (so-called static approximation). The effect of the dynamic spin fluctuations with nonzero bosonic Matsubara frequencies, which are less important in the renormalized classical regime, is considered below. In the static approximation and for the nearly constant Fermi velocity v_F in the vicinity of the Fermi momentum k_F , both the self-energy and vertices are actually functions of $i\nu_n - \varepsilon_{\mathbf{k}}$ only:

$$\Sigma_{\mathbf{k}} = \Sigma(i\nu_n - \varepsilon_{\mathbf{k}}), \quad \gamma_{\mathbf{k}}^{m_1 \dots m_n} = \gamma^{m_1 \dots m_n}(i\nu_n - \varepsilon_{\mathbf{k}}). \quad (23)$$

The integration over momenta can then be simplified by introducing an auxiliary variable $a = v_F \mathbf{q} \cdot (\mathbf{k}_F / k_F)$ (cf. Ref. 26),

$$\begin{aligned} & T \sum_{\mathbf{q}} (\gamma_{\mathbf{k}+\mathbf{q}}^{m_1 \dots m_n})^p G_{\mathbf{k}+\mathbf{q}}^n \chi_{\mathbf{q}} \\ &= \frac{AT}{4\pi M} \int_{-D}^D \frac{da}{\sqrt{a^2 + v_F^2 \xi^{-2}}} \frac{[\gamma^{m_1 \dots m_n}(\bar{\nu} - a)]^p}{[\bar{\nu} - a - \Sigma(\bar{\nu} - a) + i0]^n}, \end{aligned} \quad (24)$$

where $\bar{\nu} = \nu - \varepsilon_{\mathbf{k}}$, we have performed an analytical continuation $i\nu_n \rightarrow \nu + i0$ and restricted the integration over a by $\pm D$ to account for the effect of finite bandwidth.

To solve Eqs. (9), (10), and (15) numerically, we parametrize the energy dependence of the self-energy $\Sigma(\nu)$ and vertices $\gamma^{m_1 \dots m_n}(\nu)$ by a set of values at the points $\{\nu_r\}_{r=1}^{N_e}$ suitably chosen on the real axis (we choose $N_e \sim 800-1000$), and iterate these equations with some initial condition until the convergence is reached. In the following, we set $A=1/v_F$ for definiteness.

First, we consider the results of the solution of these equations for the s - d model. The frequency dependence of the self-energy Σ_ν and the spectral functions within the $1/z$ expansion is shown in Fig. 2; the corresponding results for the self-energy, spectral functions, and the vertex γ_ν within the $1/M$ expansion are shown in Fig. 3.

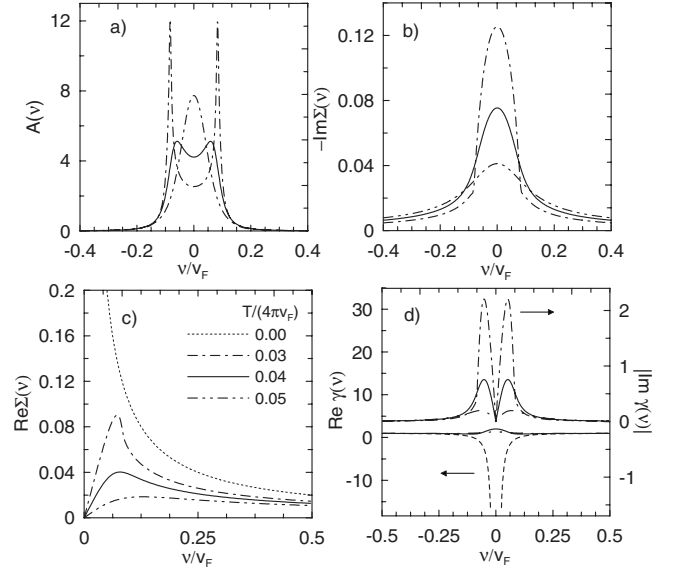


FIG. 3. (a) The spectral functions, (b) the imaginary and (c) real parts of the self-energy, and (d) the vertex function γ of the s - d model in the weak-coupling regime in the first-order $1/M$ expansion at $M=3, I=0.1v_F, D=5v_F$, and different values of temperature.

One can observe that the form of the spectral functions in $1/z$ and $1/M$ expansions is similar. In particular, we find that the imaginary part of the self-energy has a Lorentz-like form with $|\text{Im} \Sigma(0)| \sim T\xi$, and the real part of the self-energy acquires a large positive slope at the Fermi level, $\partial \text{Re} \Sigma / \partial \nu \sim T\xi^2$, so that the quasiparticle picture is invalid. With decreasing temperature, the structure of the spectral functions changes from the one-peak to two-peak form; the latter occur when the inverse correlation length $\xi^{-1} \sim I/v_F$. At lower temperatures, the electronic spectrum and corresponding Fermi surface are quasisplit due to strong magnetic fluctuations.

These results are similar to the previously obtained results for the spin-fermion model within the quasistatic approach.^{20,23,26} The results of the $1/M$ expansion for the spin-fermion model are shown in Fig. 4. To compare the results to the earlier studies and to the s - d model, we introduce the quantity Δ according to Eq. (19). At large ξ , we obtain $\Delta = [(ATJ^2/4\pi) \ln(D\xi/v_F)]^{1/2}$. This quantity approaches a constant value Δ_0 in the $T \rightarrow 0$ limit in the renormalized-classical regime; this value is the analog of the interaction I in the s - d model. The qualitative behavior of the self-energy, spectral functions, and vertices is very similar to those of Fig. 3 for the s - d model and the results of Ref. 26. In particular, the spectral functions have a two-peak form at low enough temperatures, with the peaks being, however, wider than found for the s - d model.

Now, we consider the effect of the dynamic spin fluctuations with nonzero bosonic Matsubara frequencies. In the approximation of constant Fermi velocity v_F , the self-energy and vertices depend on the difference $i\nu_n - \varepsilon_{\mathbf{k}}$ (contrary to the above discussed contribution of static spin fluctuations, it does not imply, however, the dependence of the self-energy at the real frequency axis on the difference $\nu - \varepsilon_{\mathbf{k}}$). After calculation of the self-energy at the imaginary-frequency

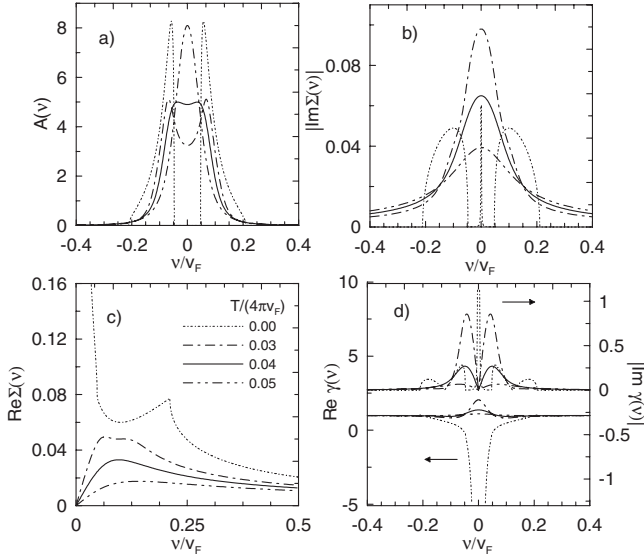


FIG. 4. The same as Fig. 3 for the spin-fermion model with $J=0.2v_F$ and $\Delta_0=0.1v_F$.

axis, we use the Padé approximants to perform analytical continuation of the results to the real axis.⁴⁰ Alternatively, one can perform calculations directly on the real axis, the results of both approaches being almost identical. The integration over momenta in Eqs. (15) can be performed similar to Eq. (24),

$$\begin{aligned}
 & T \sum_{\mathbf{q}} \sum_{i\omega_n} (\gamma_{k+\mathbf{q}}^{m_1 \dots m_n})^p G_{k+\mathbf{q}}^n \chi_{\mathbf{q}} \\
 &= \frac{AT}{4\pi M} \sum_{i\omega_n} \int_{-D}^D da \frac{f_{\omega_n}(a) [\gamma^{m_1 \dots m_n}(i\nu_n + i\omega_n - a)]^p}{[\bar{\nu}_n + i\omega_n - a - \Sigma(i\bar{\nu}_n + i\omega_n - a)]^n}, \\
 & f_{\omega_n}(a) = \frac{2}{\pi} \int_{|a|/v_F}^{D/v_F} \frac{qdq}{\sqrt{q^2 - (a/v_F)^2} \sqrt{q^2 + \xi^2 + r|\omega_n|/q}}, \quad (25)
 \end{aligned}$$

with $\bar{\nu}_n = i\nu_n - \varepsilon_{\mathbf{k}}$.

The results for the self-energy and spectral functions in the renormalized-classical regime of the effective s - d model with different bandwidths are shown in Fig. 5. Although the low-energy behavior of the self-energy and spectral functions [Figs. 5(a) and 5(b)] is similar to that found in the static approximation (Fig. 3), the self-energy at higher frequencies $\Delta_0 \ll |\nu| \ll D$ behaves as $\Sigma(\nu) \sim \nu^{2/3}$. At very high frequencies $|\nu| \gtrsim D$, the behavior of the self-energy $\Sigma(\nu) \sim 1/\nu$ is restored. The results for the spin-fermion model with the dynamic spin fluctuations are shown in Fig. 6 and have the same qualitative frequency dependence as for the effective s - d model; the low-energy behavior of the spectral functions [Figs. 6(c) and 6(d)] is close to the corresponding results of the static approximation (Fig. 4). Therefore, the effect of dynamic spin fluctuations in the renormalized-classical regime is not pronounced, and the static approximation describes correctly the low-energy behavior of the self-energy and spectral functions.

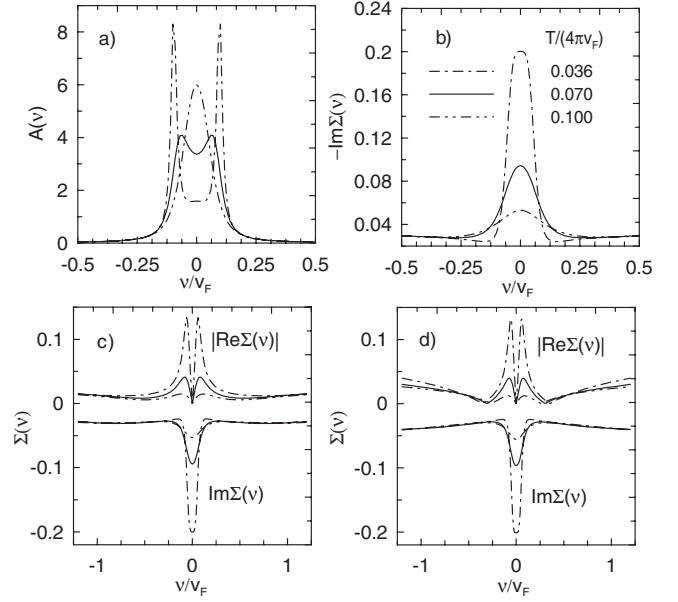


FIG. 5. (a) The spectral functions and (b) the imaginary and [(c) and (d)] real parts of the self-energy of the effective s - d model in the renormalized classical regime with account of the dynamic spin fluctuations at the bandwidth [(a)–(c)] $D=v_F$ and (d) $D=5v_F$, $I=0.1v_F$, and different values of temperature.

A treatment of the dynamic spin fluctuations with nonzero bosonic Matsubara frequencies is necessary to consider the self-energy and spectral functions in the quantum-critical regime. Although in that case the ansatz for the susceptibility (16) may not be correct because of the possible nonanalytic corrections,⁴¹ it is still interesting to investigate the self-energy and spectral functions in this regime with this ansatz to clarify the role of dynamic spin fluctuations. In the quantum-critical regime, the quantity $\Delta_0 = [(ATJ^2/4\pi)\ln(D\xi/$

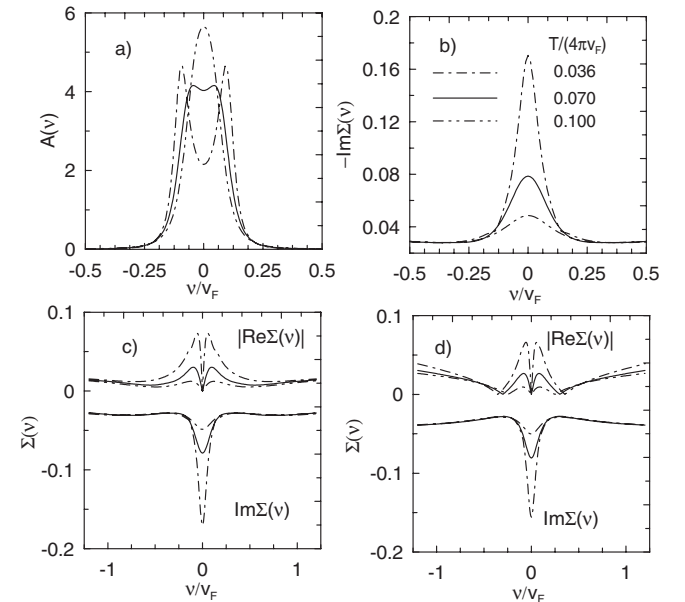


FIG. 6. The same as Fig. 5 for the spin-fermion model with $J=0.2v_F$ and $\Delta_0=0.1v_F$.

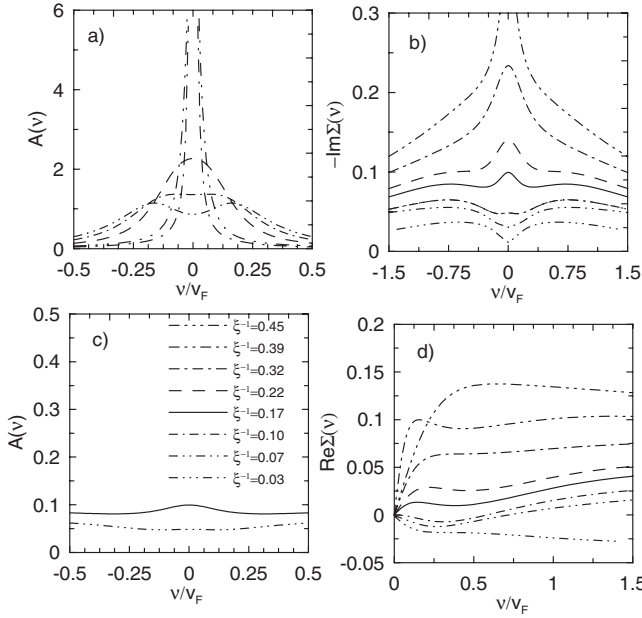


FIG. 7. [(a) and (c)] The spectral functions and the (b) imaginary and (d) real parts of the self-energy of the spin-fermion model in the quantum-critical regime for different values of the correlation length.

$v_F]$ becomes temperature dependent itself, and one has to employ additional ansatz for the temperature dependence of correlation length. According to the Hertz-Millis theory⁴² (which is valid in the absence of nonanalytical corrections to susceptibility),

$$\xi^{-1} = B(T/v_F)^{1/2}, \quad (26)$$

for definiteness we set $B=1$.

The resulting self-energy and spectral functions are shown in Fig. 7. The frequency dependence of these quantities is determined by the interplay of static and dynamic fluctuations. At small ξ^{-1} , the dynamic fluctuations dominate, the real part of the self-energy has negative slope, and the imaginary part has a minimum at the Fermi level, the spectral functions having one-peak structure, so that the quasiparticle picture is valid. However, the behavior of the self-energy $\Sigma(v) \sim v^{2/3}$ at intermediate frequencies ($Tv_F)^{1/2} \ll |v| \ll D$ leads to strong damping of the quasiparticles, similar to the charge instability case.⁴³ At larger ξ^{-1} , the static fluctuations start to dominate and the low-frequency behavior found in Ref. 26 in the quasistatic approximation is restored: the imaginary part of the self-energy acquires maximum at the Fermi level, the real part having a positive slope; this invalidates completely the quasiparticle picture. Although the two-peak structure of the spectral functions is formed at intermediate ξ^{-1} , only a structure with one broad peak survives with increasing ξ^{-1} . The observed behavior of the self-energy is also very similar to that found for the Pomeranchuk instability case in Ref. 43. This shows that the vertex corrections (which are different in the cases of charge and spin instabilities) are not too important in the quantum-critical regime.

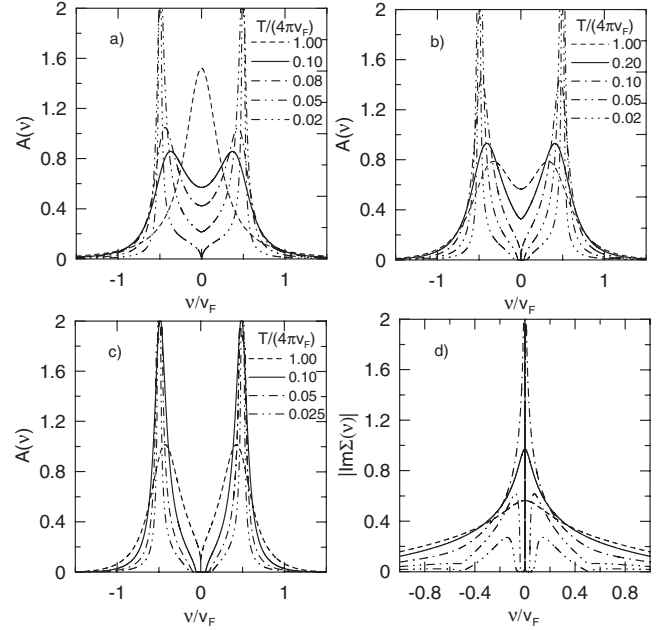


FIG. 8. The spectral functions of the classical s - d model in the intermediate-coupling regime $I=0.5v_F$ for the bandwidths (a) $D=2v_F$, (b) $D=v_F$, and (c) $D=0.7v_F$ at different low temperatures. (d) shows the imaginary part of the self-energy for $D=v_F$.

C. Low-temperature results in the intermediate-coupling regime

With increasing the interaction I in the s - d model for the nearly half-filled band, one approaches the metal-insulator transition. Although at this filling the AFM rather than the FM instability is expected in the one-band model, we consider the ferromagnetic instability, supposing that it is stabilized by the influence of the other bands in a more general multiband model.

To obtain numerical solutions in the intermediate-coupling regime, it appears necessary to use a smooth cutoff corresponding to the finite bandwidth, e.g., introducing the cutoff function

$$w(a) = \frac{1}{2} \left(1 - \tanh \frac{2|a-D|}{D} \right) \quad (27)$$

in the integration over a in Eq. (24) and extending the limits of integration from $-\infty$ to ∞ . The frequency dependence of the spectral functions $A(v)$ and the self-energy $\Sigma(v)$, obtained from the $1/z$ expansion for $D/v_F=2, 1$, and 0.7 , is shown in Fig. 8. One can see that at temperatures lower than some finite temperature T_s (i.e., at large enough ξ), the spectral functions vanish at small v , which corresponds to the magnetically induced gap or splitting of the electronic spectrum by magnetic fluctuations. The former possibility corresponds to magnetically induced metal-insulator transition, similar to that observed in manganates, while the latter fits to the weak-coupling scenario of Sec. VB. Clarification of which of the two possibilities is realized, requires further investigation. The finiteness of the temperature T_s is, however, most likely an artifact of $1/z$ expansion.

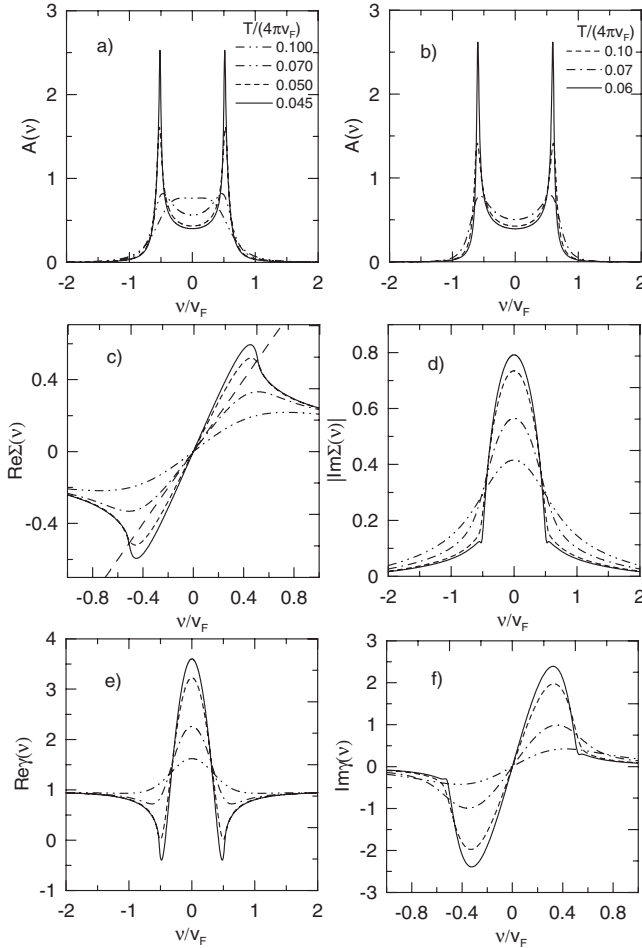


FIG. 9. The spectral functions of the classical s - d model with the bandwidths (a) $D=2v_F$ and (b) $D=v_F$ in the first-order $1/M$ expansion at $M=3$ at different low temperatures and $I=0.5v_F$. (c)–(f) show the real and imaginary parts of the self-energy and the vertex function γ for $D=2v_F$.

The results of the $1/M$ expansion for the spectral functions $A(\nu)$ and the self-energy Σ_ν , and vertices γ_ν , at the Fermi surface at $M=3$ are shown in Fig. 9. One can observe that at not too low temperatures, the results of $1/M$ expansion are similar to the results of $1/z$ expansion. At low temperatures, however, the $1/M$ expansion shows finite spectral weight at the Fermi level, additional spikes of $\text{Im} \Sigma(\nu)$ occur at $|\nu| = \nu_c \simeq \Delta_0$; at some temperature T'_s , we find $\text{Im} \Sigma(\nu_c) = 0$ and $\text{Re} \Sigma(\nu_c) = \nu_c$, so that the pole of the electronic Green's function shifts to the real axis. At $T < T'_s$, the solution to Eqs. (15) becomes nonanalytical in the upper half-plane, so that the $1/M$ expansion is not able to describe the low temperature regime. It does not exclude, however, the possibility of the magnetically-induced metal-insulator transition, discussed above. Although a small damping of electronic excitations is expected to appear in higher orders of the $1/M$ expansion, the temperature T'_s seems to correspond to a crossover to the regime with strongly coherent excitations at new preformed Fermi surfaces.

VI. CONCLUSION

We have investigated the problem of splitting of the electronic spectrum due to coupling of electronic degrees of freedom to local magnetic moments and collective magnetic modes in itinerant systems. In both regimes of weak and intermediate coupling of magnetic and electronic degrees of freedom, the spectral functions at sufficiently low temperatures have a two-peak form, arising as a presplitting of the energy spectrum. In the intermediate-coupling regime, the width of the peaks in the classical s - d model tends to zero at the temperature T'_s in the first order of the $1/M$ expansion, making the excitations at the preformed Fermi surfaces coherent at $T < T'_s$. Although a small damping of the electronic excitations is expected to arise at finite T in higher orders of the $1/M$ expansion, it is not expected to change qualitatively the form of the spectral functions. In the $1/z$ expansion, we observe the full splitting of electronic spectra and/or magnetically induced gap in the intermediate-coupling regime at sufficiently low temperatures.

The dynamic spin fluctuations do not change qualitatively the low-frequency behavior of the spectral functions in the renormalized-classical regime at weak coupling. These fluctuations are, nevertheless, important in the quantum-critical regime, where we observed a rich behavior of the spectral functions, which is determined by the interplay of static and dynamic fluctuations. The account of static fluctuations alone is not sufficient to describe correctly the spectral functions in this regime.

A generalization of the results obtained in the present paper to the quantum s - d model is of great interest. This generalization will allow one to describe analytically the formation of the Kondo resonance at the Fermi level near the metal-insulator transition in $d \rightarrow \infty$, as well as its interplay with magnetic degrees of freedom in finite-dimensional quantum Kondo lattices. Another problem, which is important for the theory of correlated magnetic metals, is the investigation of the local-moment formation and magnetic fluctuations in itinerant-electron systems (e.g., described by the Hubbard model).

ACKNOWLEDGMENTS

We are grateful to P. Igoshev for careful reading of the manuscript. The research described was supported in part by Grants No. 4640.2006.2 (Support of Scientific Schools) and No. 07-02-01264a from the Russian Basic Research Foundation.

APPENDIX: DERIVATION OF THE EQUATIONS FOR THE SELF-ENERGY AND VERTICES

In this appendix, we consider the derivation of the system of integral equations for the self-energy and vertices. Using the equation of motion (11), we obtain

$$\begin{aligned}
 H_0(\partial_x) \langle T [c_x c_y^\dagger S_a^{m_1} S_b^{m_2} S_c^{m_3} \dots] \rangle \\
 = \delta(x-y) \langle T [S_a^{m_1} S_b^{m_2} S_c^{m_3} \dots] \rangle \\
 + J \langle T [c_x c_y^\dagger (\boldsymbol{\sigma}_x) S_a^{m_1} S_b^{m_2} S_c^{m_3} \dots] \rangle, \quad (\text{A1})
 \end{aligned}$$

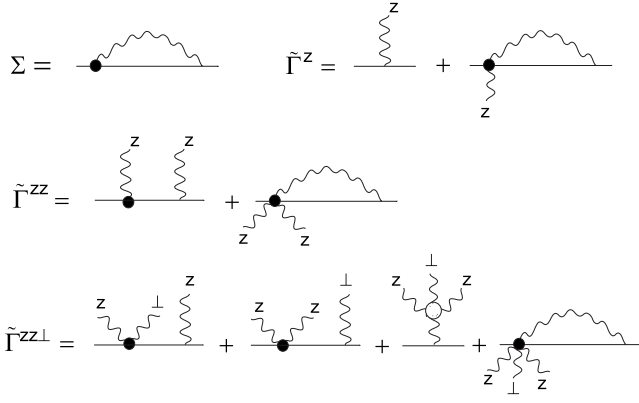


FIG. 10. Diagram representation of Eq. (A6). Solid lines correspond to the bare electronic Green functions, the black circles stand for the one-particle reducible vertices (A5), and wiggly lines denote external legs of these vertices. The dashed circles correspond to the vertex $\tilde{R}_{q_1 q_2 q_3 q_4}^{m_1 m_2 m_3 m_4}$.

where $H_0(\partial_x) = \partial_\tau + \varepsilon(\nabla)$, and x, y, a, b , and c are the space-time coordinates. Translating this to the momentum-frequency space and combining the result with the Dyson equation $G^{-1} = -(H_0 + \Sigma)$, we find

$$\begin{aligned} \Sigma_k &= TJ \sum_{q,m} \Gamma_{k;q}^m G_{k+q}^0, \\ \Gamma_{k;q_1 \dots q_n}^{m_1 \dots m_n; \sigma \sigma'} &= -G_k^{-1} \delta_{q_1 + \dots + q_n} R_{q_1 \dots q_n}^{m_1 \dots m_n} \\ &\quad - TJ \sum_{q_{n+1}, m_{n+1}, \sigma''} \Gamma_{k;q_1 \dots q_{n+1}}^{m_1 \dots m_{n+1}, \sigma \sigma''} \sigma_{\sigma'' \sigma'}^{m_{n+1}} G_{k+q_1 + \dots + q_{n+1}}^0, \end{aligned} \quad (\text{A2})$$

where $G_k^0 = (i\nu_n - \varepsilon_{\mathbf{k}})^{-1}$,

$$\begin{aligned} \Gamma_{k;q_1 \dots q_n}^{m_1 \dots m_n; \sigma \sigma'} &= -G_k^{-1} (G_{k+q_1 + \dots + q_n}^0)^{-1} \int_0^\beta d\tau \cdot d\tau_1 \dots d\tau_n \\ &\quad \times \langle T[S_{\mathbf{q}_1}^{m_1}(\tau_1) \dots S_{\mathbf{q}_n}^{m_n}(\tau_n) c_{\mathbf{k}\sigma}^\dagger(\tau) c_{\mathbf{k}+\mathbf{q}_1 + \dots + \mathbf{q}_n, \sigma'}(0)] \rangle \\ &\quad \times e^{i\nu\tau + i\omega_1 \tau_1 + \dots + i\omega_n \tau_n} \end{aligned} \quad (\text{A3})$$

are the *reducible* vertices of the interaction of an electron with n magnons,

$$R_{q_1 \dots q_n}^{m_1 \dots m_n} = \int_0^\beta d\tau_1 \dots d\tau_n e^{i\omega_1 \tau_1 + \dots + i\omega_n \tau_n} \langle T[S_{\mathbf{q}_1}^{m_1}(\tau_1) \dots S_{\mathbf{q}_n}^{m_n}(\tau_n)] \rangle \quad (\text{A4})$$

is the spin correlation function.

To obtain the equations for one-particle irreducible vertices, we first define the connected vertices via the recursive relations

$$\begin{aligned} \tilde{\Gamma}_{k;q_1 \dots q_n}^{m_1 \dots m_n; \sigma \sigma'} &= \Gamma_{k;q_1 \dots q_n}^{m_1 \dots m_n; \sigma \sigma'} + (G_k^0)^{-1} \delta_{q_1 + \dots + q_n} R_{q_1 \dots q_n}^{m_1 \dots m_n} \\ &\quad - \sum_{s=2}^{n-1} \sum_{\{I_s^n\}} \delta_{q_{i_1} + \dots + q_{i_s}} R_{q_{i_1} \dots q_{i_s}}^{m_{i_1} \dots m_{i_s}} \tilde{\Gamma}_{k;q_{i_{s+1}} \dots q_{i_n}}^{m_{i_{s+1}} \dots m_{i_n}; \sigma \sigma'}, \end{aligned} \quad (\text{A5})$$

where $I_s^n = \{i_r\}_{r=1}^s$ is the s -element ordered subset of $\{1 \dots n\}$; $\{i_r\}_{r=s+1}^n = \{1 \dots n\} \setminus I_s^n$, and the summation is taken over all subsets I_s^n . The equations for the vertices (A5) read

$$\begin{aligned} \tilde{\Gamma}_{k;q_1 \dots q_n}^{m_1 \dots m_n; \sigma \sigma'} &= TJ \sum_{m_{n+1}} \left\{ \tilde{R}_{q_1 \dots q_n, q_1 + \dots + q_n}^{m_1 \dots m_{n+1}} \sigma_{\sigma \sigma'}^{m_{n+1}} - \sum_{s=1}^{n-1} \sum_{\{I_s^n, \sigma''\}} \tilde{R}_{q_{i_1} \dots q_{i_s}, q_{i_1} + \dots + q_{i_s}}^{m_{i_1} \dots m_{i_s}, m_{n+1}} G_{k+q_{i_1} + \dots + q_{i_s}}^0 \tilde{\Gamma}_{k;q_{i_{s+1}} \dots q_{i_n}}^{m_{i_{s+1}} \dots m_{i_n}; \sigma \sigma''} \sigma_{\sigma'' \sigma'}^{m_{n+1}} \right. \\ &\quad \left. - \sum_{q_{n+1}, \sigma''} \tilde{\Gamma}_{k;q_1 \dots q_{n+1}}^{m_1 \dots m_{n+1}, \sigma \sigma''} \sigma_{\sigma'' \sigma'}^{m_{n+1}} G_{k+q_1 + \dots + q_{n+1}}^0 \right\}, \end{aligned} \quad (\text{A6})$$

where \tilde{R} denotes the connected part of R . The diagram representation of Eq. (A6) for $n=1, \dots, 3$ and Eq. (A2) for the self-energy is shown in Fig. 10.

At the next step, we express the vertices $\tilde{\Gamma}_{k;q_1 \dots q_n}^{m_1 \dots m_n}$ through the corresponding one-particle irreducible vertices $\gamma_{k;q_1 \dots q_n}^{m_1 \dots m_n}$ with the use of the Legendre transformation of the generating functional, see, e.g., Ref. 44. To the first order in $1/M$, the equations for Σ_k , γ_{k,q_1} , γ_{k,q_1}^{zz} , and $\gamma_{k,q_1 q_2}^{zz\perp}$ form a closed system, see Fig. 11. The analytical form of these equations reads (below, we omit the electronic spin indices of γ assuming that any of the equal nonzero spin components of the vertex is taken)

$$\Sigma_k = M \sum'_q \gamma_{k;q} G_{k+q} \chi_q, \quad (\text{A7})$$

$$\gamma_{k,q_1} = 1 + \sum'_{q_2} [(2-M) \gamma_{k;q_2} \gamma_{k+q_2;q_1} G_{k+q_2} + \gamma_{k;q_1,q_2}^{zz} \chi_{q_2} G_{k+q_1+q_2}], \quad (\text{A8})$$

$$\begin{aligned} \gamma_{k;q_1q_2}^{zz} = & M \sum_{q_3}' G_{k+q_1+q_2+q_3} \chi_{q_3} [\gamma_{k;q_3} \gamma_{k+q_3;q_1} \gamma_{k+q_3+q_1;q_2} G_{k+q_3} G_{k+q_3+q_1} + \gamma_{k;q_3} \gamma_{k+q_3;q_2} \gamma_{k+q_3+q_2;q_1} G_{k+q_3} G_{k+q_3+q_2} \\ & + \gamma_{k;q_1q_2q_3}^{zz\perp} + \gamma_{k;q_3} \gamma_{k+q_3;q_1q_2}^{zz} G_{k+q_3} + M \gamma_{k,q_1+q_2+q_3} \Gamma_{q_1q_2q_3}^{+-zz} \chi_{q_1+q_2+q_3}], \end{aligned} \quad (\text{A9})$$

$$\begin{aligned} \gamma_{k;q_1q_2q_3}^{zz\perp} = & M \sum_{q_4}' G_{k+q_1+q_2+q_3+q_4} \chi_{q_4} [\gamma_{k;q_4} (\gamma_{k+q_4;q_1} \gamma_{k+q_4+q_1;q_3} \gamma_{k+q_4+q_1+q_3;q_2} G_{k+q_4} G_{k+q_4+q_1} G_{k+q_4+q_1+q_3} \\ & + \gamma_{k+q_4;q_2} \gamma_{k+q_4+q_2;q_3} \gamma_{k+q_4+q_2+q_3;q_1} G_{k+q_4} G_{k+q_4+q_2} G_{k+q_4+q_2+q_3} - \gamma_{k+q_4;q_3} \gamma_{k+q_4+q_3;q_1} \gamma_{k+q_4+q_1+q_3;q_2} G_{k+q_4} G_{k+q_4+q_3} G_{k+q_4+q_3+q_1} \\ & - \gamma_{k+q_4;q_3} \gamma_{k+q_4+q_3;q_2} \gamma_{k+q_4+q_2+q_3;q_1} G_{k+q_4} G_{k+q_4+q_3} G_{k+q_4+q_3+q_1} - \gamma_{k+q_4;q_1} \gamma_{k+q_4+q_1;q_2} \gamma_{k+q_4+q_1+q_2;q_3} G_{k+q_4} G_{k+q_4+q_1} G_{k+q_4+q_1+q_2} \\ & - \gamma_{k+q_4;q_2} \gamma_{k+q_4+q_2;q_1} \gamma_{k+q_4+q_1+q_2;q_3} G_{k+q_4} G_{k+q_4+q_2} G_{k+q_4+q_1+q_2} - \gamma_{k+q_4+q_1+q_2;q_3} \gamma_{k+q_4;q_1q_2}^{zz} G_{k+q_4} G_{k+q_4+q_1+q_2} \\ & - \gamma_{k+q_4;q_3} \gamma_{k+q_4+q_3;q_1q_2}^{zz} G_{k+q_4} G_{k+q_4+q_3} - \gamma_{k+q_4;q_1q_2q_3}^{zz\perp} G_{k+q_4}) - M \gamma_{k,q_1+q_2+q_4} \Gamma_{q_1q_2q_4}^{+-zz} G_{k+q_1+q_2+q_4} \chi_{q_1+q_2+q_4} \gamma_{k,q_1+q_2+q_4} \\ & - \gamma_{k+q_1+q_2+q_4;q_3} \gamma_{k;q_1q_2q_4}^{zz\perp} G_{k+q_1+q_2+q_4}], \end{aligned} \quad (\text{A10})$$

where $\chi_q = \chi_q^z$,

$$\Gamma_{q_1q_2q_3}^{m_1m_2m_3m_4} = T J^{-2} \tilde{R}_{q_1q_2q_3,q_1+q_2+q_3} (\chi_{q_1}^{m_1} \chi_{q_2}^{m_2} \chi_{q_3}^{m_3} \chi_{q_1+q_2+q_3}^{m_4})^{-1} \quad (\text{A11})$$

is the irreducible vertex of the two-magnon interaction. In previous treatments of the spin-fermion model (see, e.g., Ref. 23), the vertex (A11) was neglected. For the flat density of states, it indeed vanishes in the limit of zero bosonic frequencies. Although it was pointed out that this vertex is singular at nonzero external frequencies and $T=0$,⁴⁵ this result is of possible relevance at finite temperatures in the quantum-critical regime only, since in the renormalized-classical and high-temperature regimes, the most important contribution to the self-energy and vertices comes from the terms with zero bosonic Matsubara frequencies. In these regimes, the vertex

(A11) may be nonnegligible for the nonconstant (especially singular) density of states. At the same time, the vertex (A11) does not vanish even for the flat density of states in the s - d model. To find this vertex, we apply the $1/M$ expansion⁴⁶ to the spin part of the model (5). To zeroth order in $1/M$, we find

$$\Gamma_{q_1q_2q_3}^{+-zz} = -2 \left[(JM)^2 T \sum_{q'} \chi_{q'} \chi_{q'+q_1+q_2} \right]^{-1}. \quad (\text{A12})$$

To perform numerical calculations, we consider two cases (see also the main text): (i) the susceptibilities χ_q are static and momentum independent, $\chi_q = \delta_{n0} \chi$, and the electronic Green's functions also do not depend on the momentum, $G_k = G_{i\nu_n}$ (high-temperature regime); (ii) the susceptibilities have a sharp maximum of the width ξ^{-1} at $q=0$, and the momentum and frequency dependence of the electronic Green's functions being arbitrary (low-temperature regime).

In both cases, we approximate in the equation for the vertex $\gamma_{k;q_1\dots q_n}^{m_1\dots m_n}$ ($n=0$ for the self-energy) the Green's functions and vertices at $q_i \neq 0$ by the corresponding quantities at the maximum total of four momentum $k+q_1+\dots+q_n$, i.e., set

$$\begin{aligned} \gamma_{k+\sum_i q_i}^{m_1\dots m_r} & \approx \gamma_{k+q_1+\dots+q_{n+1}}^{m_1\dots m_r}, \\ G_{k+\sum_i q_i} & \approx G_{k+q_1+\dots+q_{n+1}}. \end{aligned} \quad (\text{A13})$$

In addition, we use the approximation

$$\sum_{q_3} f_{q_i;q_3} \chi_{Q+q_3} \chi_{q_3} \Gamma_{q_1q_2q_3}^{+-zz} \approx f_{q_i;0} \sum_{q_3} \Gamma_{q_1q_2q_3}^{+-zz} \chi_{Q+q_3} \chi_{q_3} = -2f_{q_i;0}, \quad (\text{A14})$$

where $f_{q_i;q_3}$ is some function of electronic Green's functions and vertices, and we have taken into account that $\Gamma_{q_1q_2q_3}^{+-zz}$ depends, in fact, only on two first momenta.

Equations (A13) and (A14) are exact in regime (i) where the electronic Green's functions and vertices are momentum

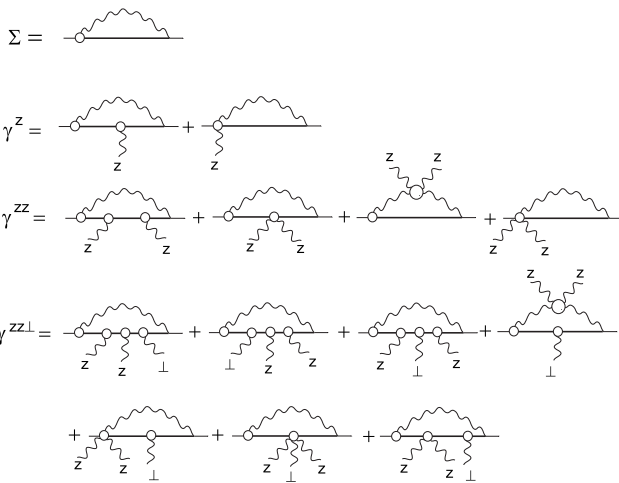


FIG. 11. Diagram representation of Eqs. (A7)–(A11). White circles stand for the one-particle irreducible vertices $\gamma_{k;q_1\dots q_n}^{m_1\dots m_n}$, dashed circles for the vertex $\Gamma_{q_1q_2q_3}^{+-zz}$ [Eq. (A11)], bold solid lines correspond to the full electronic Green function, and wiggly lines to the magnetic susceptibility χ_q .

independent and the bosonic Matsubara frequencies can be set to zero. In regime (ii), the approximation (A13) underestimates slightly the effect of magnetic correlations, but treats them qualitatively correct and becomes exact in the limit of infinite correlation length (where only vertices with the mo-

mentum $q=0$ enter). Approximation (A14) is even more accurate in regime (ii), since the product $\chi_{Q+q_3}\chi_{q_3}$ is even strongly peaked at $q_3=0$. Applying Eqs. (A13) and (A14) to Eqs. (A7) and (A10), we obtain the system of equations (15) of the main text.

- ¹J. C. Slater, Phys. Rev. **49**, 537 (1936); **49**, 931 (1936).
- ²S. V. Vonsovskii, Zh. Eksp. Teor. Fiz. **16**, 981 (1946); Sov. Phys. JETP **2**, 26 (1956); *Magnetism* (Wiley, New York, 1974).
- ³J. Kondo, Solid State Phys. **23**, 183 (1969).
- ⁴A. Hewson, *The Kondo Problem to Heavy Fermions* (Cambridge University Press, Cambridge, 1993).
- ⁵E. L. Nagaev, *Physics of Magnetic Semiconductors* (Mir, Moscow, 1983).
- ⁶E. L. Nagaev, Phys. Rep. **346**, 387 (2001).
- ⁷E. Dagotto, *Nanoscale Phase Separation and Colossal Magnetoresistance* (Springer, Berlin, 2003).
- ⁸V. Yu. Irkhin and M. I. Katsnelson, J. Phys.: Condens. Matter **2**, 7151 (1990).
- ⁹A. Anokhin, V. Yu. Irkhin, and M. I. Katsnelson, J. Phys.: Condens. Matter **3**, 1475 (1991).
- ¹⁰W. Metzner and D. Vollhardt, Phys. Rev. Lett. **62**, 324 (1989); A. Georges, G. Kotliar, W. Krauth, and M. Rozenberg, Rev. Mod. Phys. **68**, 13 (1996); G. Kotliar and D. Vollhardt, Phys. Today **57** (3), 53 (2004).
- ¹¹J.-X. Zhu, D. R. Grempel, and Q. Si, Phys. Rev. Lett. **91**, 156404 (2003); T. Ohashi, S. Suga, and N. Kawakami, J. Phys.: Condens. Matter **17**, 4547 (2005).
- ¹²V. Korenman, J. L. Murray, and R. E. Prange, Phys. Rev. B **16**, 4032 (1977); **16**, 4048 (1977); **16**, 4058 (1977).
- ¹³T. Moriya, *Spin Fluctuations in Itinerant Electron Magnetism* (Springer, Berlin, 1985).
- ¹⁴H. A. Mook, J. W. Linn, and R. M. Nicklow, Phys. Rev. Lett. **30**, 556 (1973); J. W. Linn, Phys. Rev. B **11**, 2624 (1975).
- ¹⁵S. Chakravarty, B. I. Halperin, and D. R. Nelson, Phys. Rev. B **39**, 2344 (1989); J. Vilks and A.-M. S. Tremblay, J. Phys. I **7**, 1309 (1997).
- ¹⁶A. P. Kampf and J. R. Schrieffer, Phys. Rev. B **41**, 6399 (1990); **42**, 7967 (1990).
- ¹⁷V. Yu. Irkhin and M. I. Katsnelson, J. Phys.: Condens. Matter **3**, 6439 (1991).
- ¹⁸K. Borejsza and N. Dupuis, Phys. Rev. B **69**, 085119 (2004).
- ¹⁹A. A. Katanin, A. P. Kampf, and V. Yu. Irkhin, Phys. Rev. B **71**, 085105 (2005).
- ²⁰E. Z. Kuchinskii and M. V. Sadovskii, Zh. Eksp. Teor. Fiz. **115**, 1765 (1999) [JETP **88**, 968 (1999)]; M. V. Sadovskii, Usp. Fiz. Nauk **171**, 539 (2001) [Phys. Usp. **44**, 515 (2001)]; arXiv:cond-mat/0408489 (unpublished).
- ²¹D. S. Dessau, T. Saitoh, C.-H. Park, Z.-X. Shen, P. Vaillella, N. Hamada, Y. Moritomo, and Y. Tokura, Phys. Rev. Lett. **81**, 192 (1998); T. Saitoh, D. S. Dessau, Y. Moritomo, T. Kimura, Y. Tokura, and N. Hamada, Phys. Rev. B **62**, 1039 (2000); N. Mannella, W. Yang, X. J. Zhou, H. Zheng, J. F. Mitchell, J. Zaanen, T. P. Devereaux, N. Nagaosa, Z. Hussain, and Z.-X. Shen, Nature (London) **438**, 474 (2005).
- ²²P. Monthoux, A. V. Balatsky, and D. Pines, Phys. Rev. Lett. **67**, 3448 (1991); Phys. Rev. B **46**, 14803 (1992).
- ²³J. Schmalian, D. Pines, and B. Stojkovic, Phys. Rev. Lett. **80**, 3839 (1998); Phys. Rev. B **60**, 667 (1999).
- ²⁴Ar. Abanov, A. V. Chubukov, and J. Schmalian, Adv. Phys. **52**, 119 (2003).
- ²⁵A. V. Chubukov, A. M. Finkelstein, R. Haslinger, and D. K. Morr, Phys. Rev. Lett. **90**, 077002 (2003); A. V. Chubukov, Phys. Rev. B **71**, 245123 (2005).
- ²⁶A. A. Katanin, Phys. Rev. B **72**, 035111 (2005).
- ²⁷A. O. Anokhin and V. Yu. Irkhin, Phys. Status Solidi B **165**, 129 (1991).
- ²⁸V. Yu. Irkhin and A. V. Zarubin, Eur. Phys. J. B **16**, 463 (2000); **38**, 563 (2004).
- ²⁹M. H. Hettler, A. N. Tahvildar-Zadeh, M. Jarrell, T. Pruschke, and H. R. Krishnamurthy, Phys. Rev. B **58**, R7475 (1998); C. Huscroft, M. Jarrell, Th. Maier, S. Moukouri, and A. N. Tahvildar-zadeh, Phys. Rev. Lett. **86**, 139 (2001); A. I. Lichtenstein and M. I. Katsnelson, Phys. Rev. B **62**, R9283 (2000); G. Kotliar, S. Y. Savrasov, G. Pálsson, and G. Biroli, Phys. Rev. Lett. **87**, 186401 (2001); T. A. Maier, M. Jarrell, T. Pruschke, and M. H. Hettler, Rev. Mod. Phys. **77**, 1027 (2005).
- ³⁰H. Kusunose, J. Phys. Soc. Jpn. **75**, 054713 (2006).
- ³¹C. Slezak, M. Jarrell, Th. Maier, and J. Deisz, arXiv:cond-mat/0603421 (unpublished).
- ³²A. Toschi, A. A. Katanin, and K. Held, Phys. Rev. B **75**, 045118 (2007).
- ³³A. N. Rubtsov, M. I. Katsnelson, and A. I. Lichtenstein, arXiv:cond-mat/0612196 (unpublished).
- ³⁴V. Yu. Irkhin and A. V. Zarubin, Phys. Rev. B **70**, 035116 (2004).
- ³⁵J. A. Hertz and D. M. Edwards, J. Phys. F: Met. Phys. **3**, 2174 (1973).
- ³⁶D. M. Edwards and J. A. Hertz, J. Phys. F: Met. Phys. **3**, 2191 (1973).
- ³⁷A. Auerbach, *Interacting Electrons and Quantum Magnetism* (Springer-Verlag, New York, 1994).
- ³⁸P. Igoshev, A. A. Katanin, and V. Yu. Irkhin, J. Exp. Theor. Phys. **105**, 1043 (2007).
- ³⁹A. Zagoskin, *Quantum Theory of Many-Body Systems* (Springer, New York, 1998).
- ⁴⁰H. J. Vidberg and J. W. Serene, J. Low Temp. Phys. **29**, 179 (1977).
- ⁴¹D. Belitz, T. R. Kirkpatrick, and T. Vojta, Phys. Rev. B **55**, 9452 (1997); A. V. Chubukov and D. L. Maslov, *ibid.* **68**, 155113 (2003); A. V. Chubukov, C. Pepin, and J. Rech, Phys. Rev. Lett. **92**, 147003 (2004).
- ⁴²A. J. Millis, Phys. Rev. B **48**, 7183 (1993).
- ⁴³L. Dell'Anna and W. Metzner, Phys. Rev. B **73**, 045127 (2006).
- ⁴⁴L. H. Ryder, *Quantum Field Theory* (Cambridge University Press, Cambridge, 1985).
- ⁴⁵Ar. Abanov and A. Chubukov, Phys. Rev. Lett. **93**, 255702 (2004).
- ⁴⁶A. V. Chubukov, S. Sachdev, and J. Ye, Phys. Rev. B **49**, 11919 (1994).